II International Conference on Particle-based Methods – Fundamentals and Applications
PARTICLES 2011
E. Oñate and D.R.J. Owen (Eds)

GRAIN SCALE SIMULATION OF FLOW IN A SANDSTONE SAMPLE BY USING THE MOVING PARTICLE SEMI-IMPLICIT (MPS) METHOD

LIANG-YEE CHENG[*], RICARDO GOLGHETTO DOMINGOS[♣] AND MARCIO MICHIHARU TSUKAMOTO[†]

[*]Dept. Construction Engineering, Escola Politécnica
University of São Paulo
Av. Almeida Prado, Trav. 2 No. 83, Ed. Engenharia Civil, 05508-900 São Paulo, SP, Brazil
e-mail: cheng.yee@poli.usp.br, web page: http://www.pcc.usp.br

[♣]Dept. Mining and Petroleum Engineering, Escola Politécnica
University of São Paulo
Av. Professor Melo Moraes, 2373, 05508-900 São Paulo, SP, Brazil
e-mail: golghetto@usp.br

[†]Dept. Naval Engineering Naval Architecture and Ocean Engineering, Escola Politécnica
University of São Paulo
Av. Professor Melo Moraes, 2231, 05508-900 São Paulo, SP, Brazil
email: michiharu@usp.br, web page: http://tpn.usp.br

Key words: Grain scale simulation, MPS.

Abstract. Since the grain scale modelling of flow in porous media is of great interest for the oil industry, the aim of the present research is to show an application of Moving Particle Semi-Implicit (MPS) method to the grain scale simulation of fluid flow in porous media. Geometry data obtained by a high-resolution CT scan of a reservoir sandstone sample was used as input for the simulations. The results of the simulations performed considering different resolutions are given, as well as the head loss and permeability obtained numerically.

1 INTRODUCTION

The grain scale modelling of flow in porous media is of great interest for the oil industry, since it allows the understanding of how the phase interfacial physics affect the fluid flow behaviour and macroscopic flow properties. Considering the development of new enhanced oil recovery methods, some studies on numerical approaches have been reported recently. Amount the recent contributions, Holmes et al. [1] modelled the water-oil flow in porous media by using Smooth Particle Hydrodyanamics (SPH). Despite the of the hypothetical porous media with relatively high porosity formed by spheres, the numerical results provide many insights about the relevance of surface tension on the effectiveness of the oil recovery. On the other hand, Ovaysi and Piris [2] carried out simulation based on Moving Particle

Semi-Implicit (MPS) method [3] and obtained the permeability of a sandstone sample.

The aim of the present research is to show an implementation for the grain scale simulation flow in porous media and the numerical results obtained from the simulations. For the three-dimensional modelling of the rock complex geometry and the flow inside its porous, MPS method developed for the simulation of incompressible flows was adopted. Numerical simulations were carried out employing data obtained by a high-resolution CT scan of a real reservoir sandstone sample. A pre-processing module was created to simplify the generation of the input data from the CT scan data. The results of the simulations performed considering different resolutions are also presented to investigate the impact of the microscopic scale modelling parameters on the macroscopic flow proprieties in order to achieve the compromising solution between accuracy and processing time.

2 MOVING PARTICLE SEMI-IMPLICIT (MPS) METHOD

The Moving Particle Semi-implicit (MPS) method adopted in the present study is a particle based fully lagrangian meshless method for incompressible flows. For the fluid domain, the governing equations are the continuity equation and the momentum conservation equation as follows:

$$\frac{D\rho}{Dt} = -\rho(\nabla \cdot \vec{u}) = 0 \tag{1}$$

$$\frac{D\vec{u}}{Dt} = -\frac{1}{\rho}\nabla P + \nu\nabla^2\vec{u} + \vec{f} \tag{2}$$

where ρ is the fluid density, $\vec{u}$ is the velocity vector, P is the pressure, ν is the kinematic viscosity and $\vec{f}$ accounts for other accelerations.

All operators are represented by particle interaction models based on the weight function which depends on the particles relative positions:

$$w(r) = \begin{cases} \frac{r_e}{r} - 1, & (r < r_e) \\ 0, & (r < r_e) \end{cases}, \tag{3}$$

where r is the distance between two particles and r_e is the effective radius, which limits the region where interaction between particles occurs.

The gradient vector and the Laplacian operators are defined as functions of the relative positions between the particles. Whereas a scalar function ϕ, the gradient vector and the Lapleacian of a particle i, considering the neighboring particles j, are represented by Eqs. (4) and (5). The gradient vector used in this study is the formulation proposed by Tanaka and Masunaga [4].

$$\langle\nabla\phi\rangle_i = \frac{d}{pnd^0}\sum_{i\neq j}\left[\frac{(\phi_j+\phi_i)}{|\vec{r}_j-\vec{r}_i|^2}(\vec{r}_j-\vec{r}_i)w(|\vec{r}_j-\vec{r}_i|)\right], \tag{4}$$

$$\langle\nabla^2\phi\rangle_i = \frac{2d}{pnd^0\lambda}\sum_{i\neq j}(\phi_j-\phi_i)w(|\vec{r}_j-\vec{r}_i|) \tag{5}$$

where d is the number of spatial dimensions, r_i and r_j are, respectively, the position vector of the particles i and j, λ is a parameter that represents the growth of variance and may be calculated using the Eq. (6):

$$\lambda = \frac{\sum_{j \neq i} |\vec{r}_j - \vec{r}_i|^2 w(|\vec{r}_j - \vec{r}_i|)}{\sum_{j \neq i} w(|\vec{r}_j - \vec{r}_i|)}. \quad (6)$$

The particle number density (pnd), calculated by Eq. (7), is proportional to the density and its initial value pnd^0 is used to ensure the condition of incompressibility of the flow.

$$pnd = \sum_{j \neq i} w(|\vec{r}_j - \vec{r}_i|) \quad (7)$$

The MPS method is based on a semi-implicit algorithm where the pressure is calculated implicitly and all other terms such as gravity and viscosity are calculated explicitly. The Poisson's equation can be deducted from the continuity equation and the pressure gradient:

$$\langle \nabla^2 P \rangle_i^{t+\Delta t} = -\frac{\rho}{\Delta t^2} \frac{pnd_i^* - pnd^0}{pnd^0} \quad (8)$$

Where, pnd^* is the particle number density explicitly calculated. The term of the left can be dicretized using the Laplacian model, leading to a system of linear equations.

Particles are considered as free surface one when their pnd are smaller than ($\beta \cdot pnd^0$). According to Koshizuka and Oka [3], β may vary between 0.80 and 0.99.

Rigid walls are discretized as particles with no motion beneath the wall particles. Two layers of dummy particles are placed at the side that has no contact with the fluid to maintain the correct particle number density estimation.

As inflow boundary condition, fluid particles are injected to the domain by moving wall particles with their dummies at a constant velocity. When they displace a distance equal to the particle size, these wall particles are replaced by fluid particles. At the same time, the position of wall and their dummies are shifted back to their initial location restarting the loop.

For two-dimensional cases analyzed herein, r_e was set to $2.1l_0$, where l_0 is the initial distance between particles, to calculate pressure gradient and the particle number density. r_e is $4.0l_0$ to cases involving the Laplacian operator.

3 CASE OF STUDY

3.1 THE SANDSTONE SAMPLE

Numerical simulations have been carried out employing a real porous rock geometry, which has been obtained by a high-resolution CT scan of a reservoir sandstone sample whose porosity is 18.2%. The dimension of the sample is 1.0 x 1.0 x 1.0 mm. The CT scan generated data set of 300 x 300 x 300 points. In order to simplify the manipulation of the huge amount of the data, a pre-processing module has been created to simplify the conversion of the CT scan data to the input data for the numerical simulations. Fig. 1 shows a view of the complex networks of the porous inside the sandstone sample generated from the high-resolution CT scan data.

Figure 1: Visualization of the pores of the 1.0x1.0x1.0 mm sandstone sample.

3.2 THE PRE-PROCESSING

The original CT scan data have identified only two regions: solid and void. To reduce the computational cost of the simulation, the resolution of the sandstone sample was reduced from 300 pts/mm to 50, 60 and 100 pts/mm. This was done by checking the most common particle type within cubes of 6, 5 and 3 points of side length, respectively. As the first step of pre-processing, points on void regions are converted into fluid particles. As the MPS method uses wall and dummies particles to model the solid surfaces, the pre-processor identify wall and dummy particles by setting a radius to check the status of a point and it neighbours. If all of the neighbour points inside the checking range are solids ones, it will be converted to a dummy particle; on the contrary it will be converted as a wall particle. Figure 2 shows a section view of the model in the 3 resolutions. The longitudinal section plan is set at 1/3 of the width of the sample because this is the position that provides good visualization of the flow inside the complex network of porous. Tab. 1 shows quantity of particles and absolute porosity of each model.

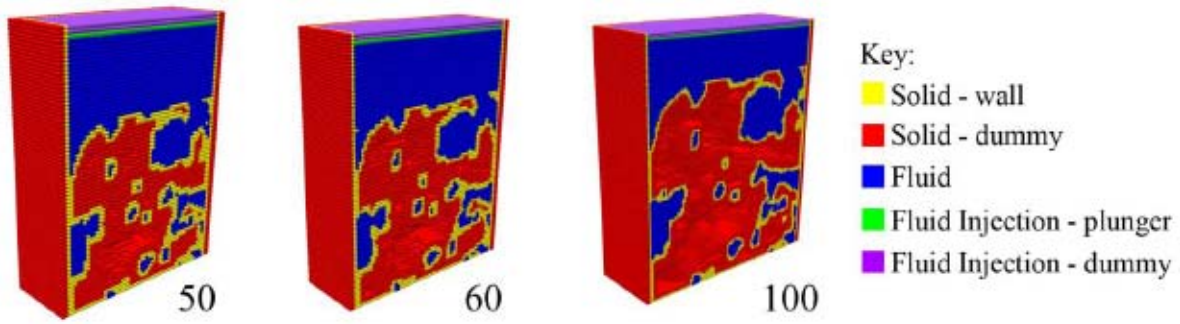

(a) (b) (c)

Figure 2: Section-view of the simulated model with 50 pts/mm (a), 60 pts/mm (b) and 100 pts/mm (c) resolutions.

Table 1: Quantity of particles and absolute porosity of each model.

Resolution [pts/mm]	Total number of particles	Absolute porosity
50	215873	0.1817
60	325394	0.1818
100	1012920	0.1827

To ensure unidirectional flow, solid walls were added to the lateral faces of the models. Also, to simulate the inflow of fluid, transition regions of 0.20, 1.33 and 0.10 mm were added in the upstream sides of the simulation models of 50, 60 and 100 pts/mm, respectively, and inflow boundary condition is set on the top of the transitions regions.

The simulated fluid is water, with a density of 10^3 kg/m^3 and a viscosity of 10^{-3} Pa.s, and it was injected with a velocity of 0.0125 m/s.

4 NUMERICAL RESULTS

4.1 PRESSURE LOSS

Simulations for the three resolutions were carried out with time step of 10^{-6} s and their results were used to calculate head loss and permeability. Figure 3 gives the snapshots of the flow and the pressure distribution for four different instant t=0.0125, 0.0250, 0.0375 and 0.0500 s. The distribution of the injected fluid (cyan colour particles), gives good insight of how the flow advances through the complex network of pores. Also, for t=0.05 s, when the flow already achieved steady state, the fluid particles originally presented in the model (blue colour particles) entrapped on the left side of the section clearly show the blocking effects of the side walls used to assure unidirectional flow, and call for more carefully interpretation of the computed permeability. On the other hand, the sequence of the pressure distributions shows that quite stable computation was obtained in this case.

More detailed numerical results at t=0.05 s of the case with 100 pts/mm resolution is illustrated in Fig. 4, which provides three sections views of pressure distribution inside the

sandstone sample. The longitudinal section plans are located at 0.25 mm, 0.50 mm and 0.75 mm from the lateral face of the sample. These section views show that a smoothly varying pressure distribution was obtained in all the pores of the model.

Figure 5 shows the time series of the computed pressure at the entrance of the sample for the three cases. Instead of starting from zero pressure, as observed in the cases with 50 pts/mm and 100 pts/mm, a very high pressure was computed on the case with 60 pts/mm resolution. Perhaps it is caused by some unstable computation in the beginning of the simulation, but despite of the difference, the time series of all the three cases converge quickly to 2746 Pa, 2859 Pa and 1081 Pa for 50 pts/mm, 60 pts/mm and 100 pts/mm, respectively, with small oscillation around the mean values. Despite the pressure drop of the case with 60 pts/mm is slightly higher than the case of 50 pts/mm, the pressure drop decreases drastically for the case of 100 pts/mm showing the effect of the spatial resolution caused mainly by the blocking of particles in narrower pores.

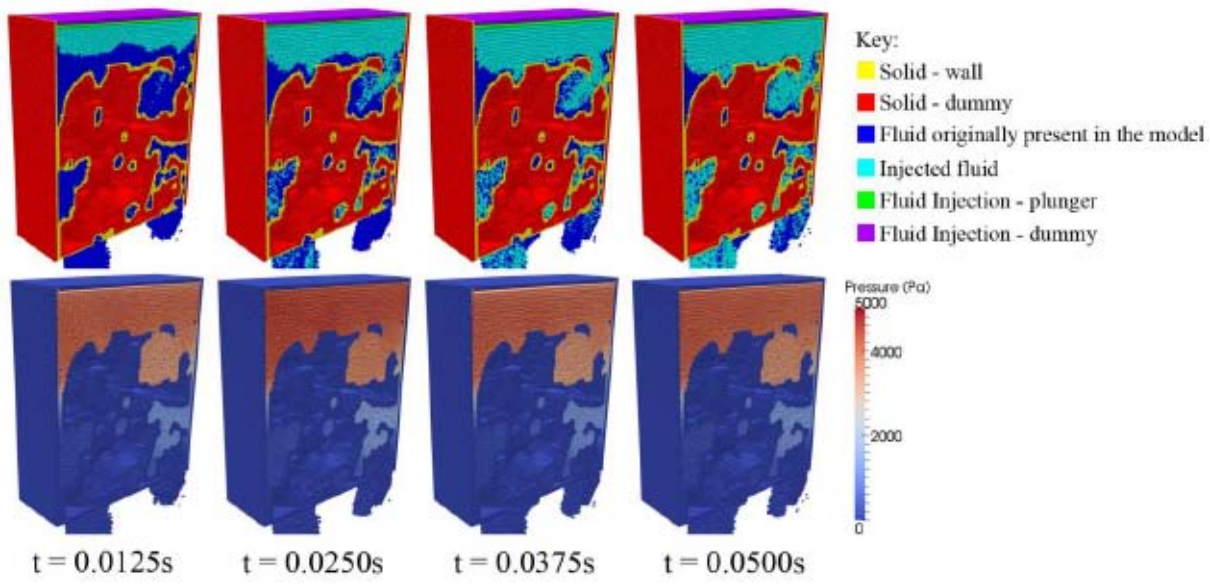

Figure 3: Snapshots of the flow and pressure distribution obtained from the simulation of the model with 100 pts/mm resolution.

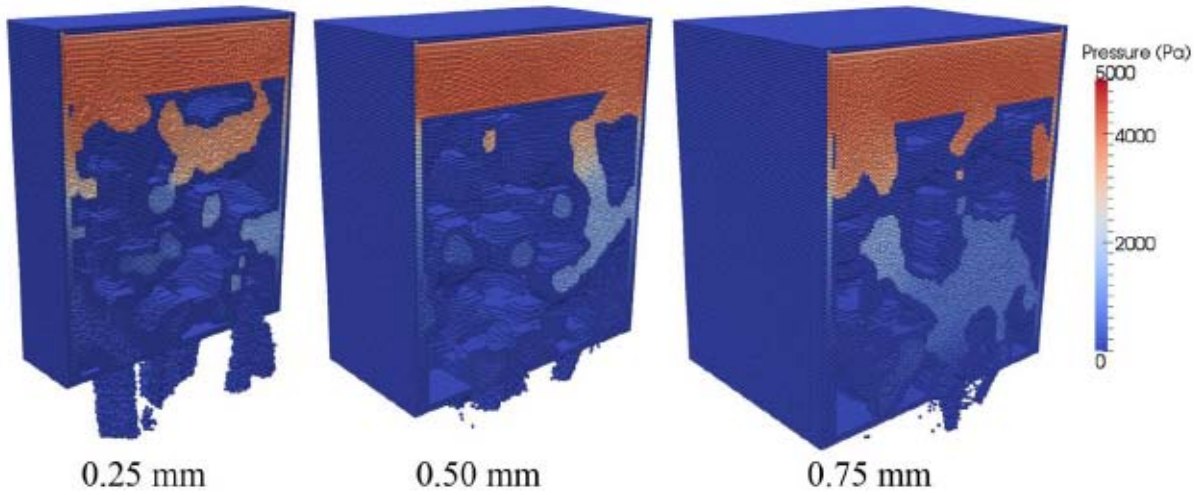

Figure 4: Longitudinal cross-sections at $\frac{1}{4}$, $\frac{1}{2}$, and $\frac{3}{4}$ of the cubic sample of the sandstone, showing the pressure distribution at 0.05 s obtained by the model of 100 pts/mm.

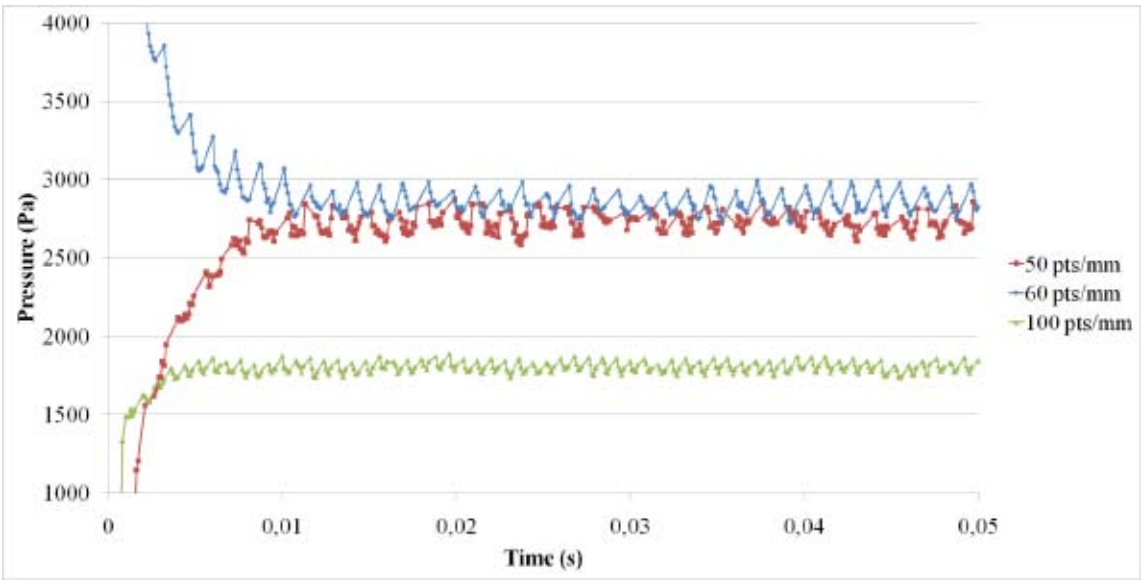

Figure 5: Pressure at the entrance of the sample through time for each tested resolution.

The pressure drop between the entrance and the exit of the sample was used to calculate the head loss and permeability of the sandstone. In this study, as the pressure at exit of the sample is set to zero, the pressure drop is equal to the pressure at the entrance of the block. A method for calculating pressure drop analytically is presented in the next section.

4.2 PERMEABILITY

The permeability can be determined by Darcy's law and it is given by:

$$k = Q\frac{\mu \cdot L}{\Delta P \cdot A} \tag{9}$$

where k is the permeability, Q is the volumetric flow, μ is the viscosity, L is the length of sample along flow direction, ΔP is the pressure drop and A is the cross-sectional area of the sample.

Since flow is the product of velocity and area, this can be simplified into:

$$k = V_S\frac{\mu \cdot L}{\Delta P} \tag{10}$$

where V_s is the superficial velocity given by:

$$V_s = \frac{Q}{A} \tag{11}$$

where Q is the volumetric flow and A is the area of the cross-section of the sample.

Head Loss can be estimated by the Bernoulli's equation. By neglecting the head loss due to the potential and kinetic components, we have:

$$\Delta H = \frac{\Delta P}{\rho \cdot g} \tag{12}$$

where g is the gravity acceleration.

From the computed pressure drops shown in the previous subsection, the computed values of head loss and permeability of the sandstone sample are given in Tab. 2.

Table 2: Computed pressure drop, head loss and permeability.

Resolution [pts/mm]	Δp [Pa]	ΔH (m)	k (mD)
50	2746	0.28	4612
60	2859	0.29	4430
100	1801	0.18	7032

4.3 VALIDATION

In order to check the magnitude of the results obtained by the numerical simulations, the pressure drop was estimated analytically by using Ergun equation:

$$f_P = \frac{150}{Re_P} + 1.75 \tag{13}$$

Where f_p is the friction factor and Re_p is the Reynolds number for porous media. Both are calculated as follow:

$$f_P = \frac{\Delta P \cdot D_{GE} \cdot \varepsilon^3}{\rho \cdot V_S^2 \cdot (1-\varepsilon) \cdot L} \tag{14}$$

$$Re_P = \frac{\rho \cdot V_s \cdot D_{GE}}{\mu \cdot (1-\varepsilon)} \tag{15}$$

where D_{GE} is the equivalent grain diameter, ε is the porosity of the sample.

Combining Eqs. (13), (14) and (15), we have:

$$\Delta P = 150\frac{\mu \cdot (1-\varepsilon)^2 \cdot V_S \cdot L}{D_{GE}^2 \cdot \varepsilon^3} + 1.75\frac{\rho \cdot V_S^2 \cdot (1-\varepsilon) \cdot L}{D_{GE} \cdot \varepsilon^3} \tag{16}$$

To estimate the equivalent grain diameter, it is assumed that they are spheres. Firstly, a

cross-section of the sample is chosen, and then its solid area is measured. Then, the number of grains inside the cross-section is obtained. Then, the average area of the grain is calculated, which will lead to the average diameter used as D_{GE}. Figure 6 illustrates the cross-section that was used to estimate the equivalent grain diameter of the sample used in this study.

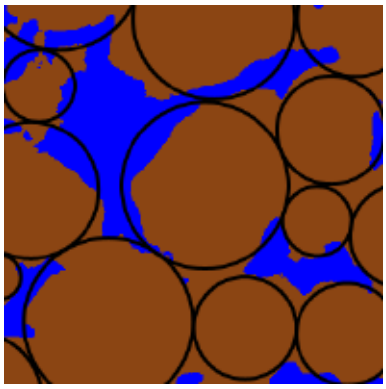

Figure 6: Cross-section used to estimate the equivalent grain diameter of the sample.

The value of the pressure drop obtained analytical is 2035 Pa. For head loss it is 0.21 m and the analytically estimated permeability is 6143 mD. The results of the analytical estimation agree relatively well with the numerical results of the model with 100 pts/mm, which is the case with highest resolution simulated in the present study.

Moreover, the order of magnitude of permeability matches with those obtained by Ovausi and Piri [2], which used a sandstone sample of 22.2% porosity, and obtained permeability of 4250 mD for a sample of 1.02 mm x 1.02 mm x 1.02 mm (300 x 3000x 300 voxels), and 7380 mD for a 0.38 mm x 0.38 mm x 0.38 mm. According to [2], the values of permeability of the 22.2% porosity sandstone obtained by using Lattice-Boltzmann is 2220 mD and by using a reconstructed pore network is 3640 mD.

5 CONCLUDING REMARKS

In the present work, grain scale simulations of flow in porous media were carried out using CT scan data of a sample of reservoir sandstone which is modelled by Moving Particle Semi-Implicit (MPS) method. For the assessment of the pressure drop, head loss and permeability, there different spatial resolutions were considered.

The numerical results shows entrapping of some fluid particle, due to the rigid walls placed on the sides of the model to assure the unidirectional flow, might affect the calculation and might require the use of a larger representative elementary volume. Nevertheless, the values computed by the present study show relatively good agreement with the analytical estimation and are consistent when compared to the results available in the literature.

In this way, the numerical method used in the present study is effective for the study of grain scale media and, as suggested by Ovaysi and Piti [2], more detailed studies are necessary to verify the convergence of the numerical results, as well as the validation through the experimental measurements.

ACKNOWLEDGMENTS

The author would like to express their gratitude to PETROBRAS for the financial support to the research.

REFERENCES

[1] Holmes DW, Williams JR, Tilke P. Smooth Particle Hydrodynamics for grain scale multiphase fluid simulation. In Proceedings of the International Conference on Particle-Based Methods Fundamentals and Applications (Particle 2009); 2009; Barcelona.

[2] Ovaysi S, Piri M. Direct pore-level modeling of incompressible fluid flow in porous media. Journal of Computational Physics. 2010: p. 7456-7476.

[3] Koshizuka S, Oka Y. Moving-Particle Semi-Implicit Method for fragmentation of incompressible fluid. Nuclear Science and Engineering. 1996; 123: p. 421-434.

[4] Tanaka M, Masunaga T. Stabilization and smoothing of pressure in MPS method by Quasi-Compressibility. Journal of Computational Physics. 2010;: p. 4279-4290.